

# Characterization of a Commercial Hyperbranched Aliphatic Polyester Based on 2,2-Bis(methylol)propionic Acid

Ema Žagar\* and Majda Žigon

National Institute of Chemistry, P.O. Box 3430, Hajdrihova 19, SI-1000 Ljubljana, Slovenia

Received July 8, 2002; Revised Manuscript Received October 15, 2002

**ABSTRACT:** A fourth generation hyperbranched polyester polyol based on bis-MPA and a PP50 core molecule (Boltorn H40) as well as its fractions obtained by preparative SEC were characterized with respect to composition, molar mass, and structure using NMR, SEC–MALS, ESI–MS, and DSC techniques. The content of dendritic units and the degree of branching (DB) are significantly lower than expected for a random polymerization, thus indicating that the hydroxyl groups in the linear repeat units are less reactive than those in terminal repeat units. The main side reaction in the synthesis of Boltorn H40 is deactivation of the bis-MPA carboxyl groups leading to structures without a core molecule. This side reaction influences mainly  $\bar{M}_n$ , and to a lesser degree the  $\bar{M}_w$  value of Boltorn H40. Furthermore, some of the hydroxyl groups react to ether groups. Etherification as a side reaction is of minor importance since the content of ether groups is below 1%. The obtained results indicate that despite deactivation of carboxyl groups of bis-MPA, the use of the PP50 core molecule in the polycondensation of bis-MPA permits control of the molar mass and polydispersity index, whereas the DB is not influenced. The  $\bar{M}_w$  of Boltorn H40 is comparable to, and  $\bar{M}_n$  is significantly lower than, the theoretical molar mass of dendritic poly-(bis-MPA) with a PP50 core molecule.

## 1. Introduction

Highly branched dendritic multifunctional polymers with unique molecular architecture, i.e., dendrimers and hyperbranched polymers, have attracted considerable and increasing interest during recent years. Their properties are different from those of linear polymers of the same molar mass (less flexibility, lower entanglement degree, a significant chain-end effect, lower viscosity in solution and in the molten state, high solubility in common solvents, a different relationship between hydrodynamic volume and molar mass, and a different origin of the glass transition temperature).<sup>1–6</sup> Well-defined monodisperse perfectly branched structures are characteristic of dendrimers, which consist of branch, i.e., dendritic repeat units, and unreacted terminal repeat units.<sup>1–5</sup> Regardless of a convergent or divergent synthetic route, each generation is built up step-by-step with many protection and deprotection synthetic and purification steps, which makes large-scale production difficult. On the other hand, hyperbranched polymers<sup>5–9</sup> are more simple to produce on a large scale via one-pot synthesis. However, this simplified procedure yields fewer regular structures and very broad molar mass distributions. The molar mass and polydispersity index (PDI) of a hyperbranched polymer depend on the monomer functional group conversion ( $p$ ) as well as its functionality. Hyperbranched polymers consist not only of dendritic and terminal repeat units but also of linear ones with one unreacted functional group. Linear units are regarded as defects in their branched structures. The branching perfection of AB<sub>2</sub> systems is characterized by an average degree of branching (DB), which is defined by Fréchet<sup>10</sup> as

$$DB = \frac{D + T}{D + L + T} \quad (1)$$

where  $D$ ,  $L$ , and  $T$  are the fractions of dendritic, linear, and terminal repeat units, respectively. DB = 1 for a

perfect dendrimer and is <1 for hyperbranched polymers. Frey et al.<sup>11</sup> have proposed another definition, where the number of actually existing growth directions is compared to the maximum possible number of growth directions in AB<sub>2</sub> systems (eq 2).

$$DB = \frac{2D}{2D + L} \quad (2)$$

According to the later definition the DB values range between 0 for the linear polymer and 1 for the perfect dendrimer structure. The DB in hyperbranched polymers formed by a random polymerization of AB<sub>2</sub> monomers or by a co-condensation of a core molecule B<sub>*f*</sub> (*f* being the core functionality) with AB<sub>2</sub> monomers may not exceed a value of 0.5. Frey et al.<sup>12</sup> analyzed the DB of hyperbranched polymers on the basis of kinetic considerations in order to follow the evolution of individual repeat units and the DB via conversion. They showed that the expression for DB (eq 2) in the case of a random one-pot AB<sub>2</sub> polycondensation exhibits the same conversion dependence as a branching parameter  $\alpha$  defined by Flory.<sup>13</sup> Experimentally and theoretically it was shown that the DB of hyperbranched polymer can be enhanced by (i) a synthetic technique where monomers AB<sub>*x*</sub> are slowly, portion by portion, added to the core molecules B<sub>*f*</sub> in solution (core dilution/slow addition technique),<sup>12,14</sup> (ii) activation of the second B group of AB<sub>2</sub> monomers after the reaction of the first B group,<sup>11</sup> and (iii) polymerization of the prefabricated perfect dendrons.<sup>15</sup>

Most studies of the dendritic and hyperbranched aliphatic polyesters based on 2,2-bis(methylol)propionic acid (bis-MPA) have been focused on their synthesis. Hult et al.<sup>7,9,17–19</sup> investigated the kinetics of the formation of poly(bis-MPA) with and without the core molecule as well as the structure buildup. They reported a pseudo-one-step reaction where stoichiometric fractions of bis-MPA as the AB<sub>2</sub> monomer, corresponding to each

generation, were added successively to tris(methylol)propane as the B<sub>3</sub> core molecule under acidic catalysis.

The relative molar mass averages of hyperbranched poly(bis-MPA) are usually determined by size exclusion chromatography (SEC) in different solvents (tetrahydrofuran, THF;<sup>17–21</sup> *N,N*-dimethylformamide, DMF<sup>22,23</sup>) using calibration with various polymer standards. The absolute number-average molar masses ( $\overline{M}_n$ ) of hyperbranched poly(bis-MPA) with tris(methylol)propane or ethoxylated Pentaerythritol (PP50) core molecule were calculated from <sup>1</sup>H NMR spectra and experimentally determined by vapor pressure osmometry (VPO).<sup>22</sup> The absolute weight-average molar masses ( $\overline{M}_w$ ) of these polyesters have not yet been reported.

The number-average degree of polymerization ( $\overline{DP}_n$ ) of hyperbranched polyester polyols depends on the conversion of individual functional groups and is expressed by the number of molecules at the beginning of the reaction ( $N_0$  at time  $t = 0$ ), and the number of molecules in the reaction mixture at a given conversion ( $N_t$  at time  $t$ ) (eq 3).<sup>24</sup>

$$\overline{DP}_n = \frac{1}{1-p} = \frac{N_0}{N_t} \quad (3)$$

If the condensation reaction takes place only between the carboxyl (A) and hydroxyl (B) groups of bis-MPA (AB<sub>2</sub>) forming an ester (AB) bond upon intermolecular reaction, then the  $\overline{DP}_n$  of poly(bis-MPA) sample can be calculated from its <sup>1</sup>H NMR spectrum, since the number of molecules at the beginning of the reaction (eq 4) and at a given conversion (eq 5) can be determined from the integrals of the signals corresponding to B (–CH<sub>2</sub>OH) and AB (–CH<sub>2</sub>OR) groups.<sup>22</sup>

$$N_0 = \frac{1}{2}(N(B) + N(AB)) \quad (4)$$

$$N_t = \frac{1}{2}(N(B) - N(AB)) \quad (5)$$

Substitution of eqs 4 and 5 into eq 3 yields eq 6.

$$(\overline{DP}_n)_{\text{NMR}} = \frac{N(B) + N(AB)}{N(B) - N(AB)} \quad (6)$$

When a core molecule B<sub>f</sub> with a functionality  $f$  higher than 2 (in the case of AB<sub>2</sub>), is introduced into the reaction mixture, the number of B groups will be higher compared to the number of molecules added. Therefore, eq 6 has to be corrected for the overestimated B groups as shown by Frey et al. (eq 7).<sup>22</sup>

$$(\overline{DP}_n)_{\text{NMR}} = \frac{N(B) + N(AB) - (f-2)N_{\text{core}}}{N(B) - N(AB) - (f-2)N_{\text{core}}} \quad (7)$$

The number of core molecules  $N_{\text{core}}$  is usually known in such experiments or can be calculated from the monomer/core ratio.

One possible side reaction, that can take place during polycondensation of bis-MPA monomers is an intramolecular reaction between a B group and the A focal group of acid dendritic unit, where the quaternary carbon is attached to an unreacted A group and two reacted B groups. This side reaction results in formation of the cyclic structures. Cyclic structures can be also formed when two hydroxyl groups react intramolecularly to

form an ether bond. Etherification may occur also intermolecularly leading to the formation of cross-linked structures and subsequently to gelation. These side reactions influence the molar mass distribution and the average degree of polymerization  $\overline{DP}_n$  of the final product.

The role of cyclization in poly(bis-MPA) hyperbranched polyesters without the core molecule was studied by ESI/FT MS<sup>25</sup> and with the core molecule tris(methylol)propane and PP50 by MALDI–TOF.<sup>22</sup> The mass spectra of poly(bis-MPA) show peaks that are characterized by a mass 18 g/mol less than the set of peaks originating from the regular polymer structure. The extent of cyclization ( $\xi$ ) through ester bonds, i.e., the number of cyclic molecules ( $N_{\text{cycles}}$ ) compared to the total number of molecules in the mixture  $N$  (eq 8), can be determined from  $\overline{DP}_n$  measured by absolute methods (i.e., VPO) and  $(\overline{DP}_n)_{\text{NMR}}$  obtained from <sup>1</sup>H NMR spectra (eq 6 or 7).

$$\xi = \frac{N_{\text{cycles}}}{N} = \frac{N - N_{\text{NMR}}}{N} = 1 - \frac{\overline{DP}_n}{(\overline{DP}_n)_{\text{NMR}}} \quad (8)$$

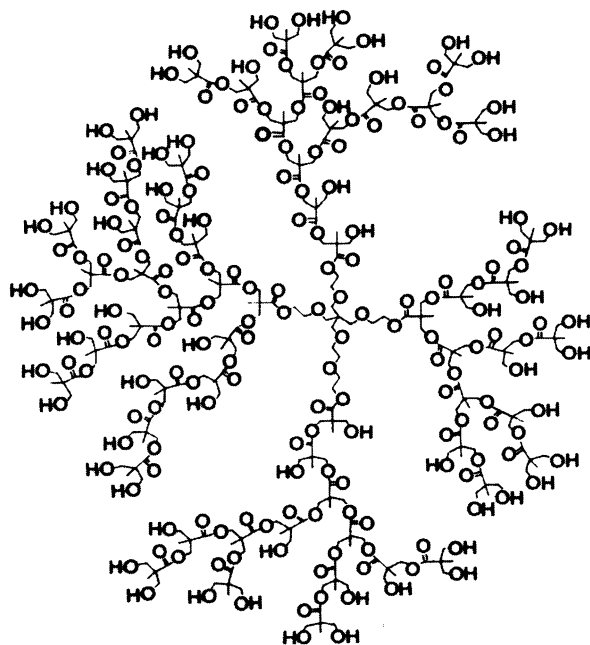
$$N = N_0/\overline{DP}_n, \quad N_{\text{NMR}} = N_0/(\overline{DP}_n)_{\text{NMR}}, \quad \text{and}$$

$$N_0 = \text{initial number of monomer molecules}^{22}$$

The portion of cyclic structures increases with increasing carboxyl group conversion and with increasing theoretical generation; in the latter case, it increases as a consequence of increasing fraction of deactivated carboxyl groups. At a given conversion, the fraction of cyclic structures in polyester without the core molecule increases with increasing molar mass,<sup>25</sup> whereas in polyester with the core molecule it decreases.<sup>22</sup> Drastically limited molar mass averages of poly(bis-MPA) hyperbranched polyesters were explained by intramolecular cyclization since it competes with the desired intermolecular reaction.<sup>22</sup>

Since the physical properties of hyperbranched polymers under application and processing conditions crucially depend on the average molar mass, molar mass distribution, degree of branching, structure (acyclic, cyclic), and composition, the aim of our work was to determine these parameters for a commercial fourth generation Boltorn H40 hyperbranched aliphatic polyester polyol based on bis-MPA and core molecule PP50 (denoted as H40, Scheme 1). We analyzed the entire sample and fractions obtained by preparative SEC in *N,N*-dimethylacetamide (DMAc) using NMR spectroscopy and size exclusion chromatography coupled to a light scattering photometer (SEC–MALS). The composition was determined by <sup>13</sup>C NMR spectroscopy under quantitative experimental conditions. Experimentally determined DB values using eqs 1 and 2 were compared to the branching coefficient obtained from the conversion of carboxyl groups of bis-MPA ( $\alpha = p_A/2$ ).<sup>13</sup> The number-average molar mass ( $\overline{M}_n$ ), the fraction of deactivated bis-MPA carboxyl groups, and the fraction of ether groups were evaluated from NMR spectra, whereas  $\overline{M}_w$ ,  $\overline{M}_n$ , and PDI were experimentally determined by SEC–MALS. The extent of cyclization through ester bonds was evaluated by comparing experimentally determined  $\overline{DP}_n$  using SEC–MALS and  $\overline{DP}_n$  calculated from <sup>1</sup>H NMR and by the ESI–MS technique.

**Scheme 1. Schematic Representation of the Hyperbranched Polyester Polyol Based on bis-MPA and the PP50 Core Molecule**



## 2. Experimental Section

**2.1. Materials.** A commercial fourth-generation hydroxy-functional hyperbranched polyester polyol was synthesized via pseudo-generation-wise addition of bis-MPA as the AB<sub>2</sub> monomer to ethoxylated Pentaerythritol (PP50) as the B<sub>4</sub> core molecule; the trade name is BOLTORN H40 (Perstorp Specialty Chemicals AB). We denote the sample H40. H40 as an ideal dendrimer would theoretically have 64 primary hydroxyl groups and a molar mass of 7316 g mol<sup>-1</sup>. It is delivered in pellets and is an amorphous solid at room temperature. Its specifications are the following:<sup>26</sup> hydroxyl number is 470–500 mg KOH g<sup>-1</sup>, acid number is 7–11 mg KOH g<sup>-1</sup>,  $\bar{M}_w = 5100$  g mol<sup>-1</sup>, PDI ( $\bar{M}_w/\bar{M}_n$ ) = 1.8 (determined by SEC in 0.2% LiBr/DMF using poly(ethylene glycol) standards), viscosity (110 °C, 30 s<sup>-1</sup>) is 110 Pa s, and the glass transition temperature is  $T_g = 40$  °C.

**2.2. Characterization.** The SEC–MALS measurements were performed at 25 °C using a Hewlett-Packard pump series 1100 coupled to a Dawn-DSP laser photometer equipped with an He–Ne laser ( $\lambda_0 = 633$  nm) and to an Optilab-DSP interferometric refractometer (DR) (both instruments are from Wyatt Technology Corp.). Separations were carried out using (i) a PLgel 5  $\mu$ m Mixed-D column (300 mm length and 7.5 mm i.d.) with a precolumn in *N,N*-dimethylacetamide (DMAc, Aldrich) and DMAc with added LiBr (Aldrich) in concentration of 0.7% and (ii) two Mixed-D (Polymer Laboratories, Ltd) columns with a precolumn in a mixture of tetrahydrofuran (THF, Fluka) and methanol (MeOH, Merck) in a volume ratio of 9:1. The PLgel Mixed-D column contains a mixture of individual pore size materials, accurately blended to cover a range of molar masses from 200 g mol<sup>-1</sup> to 400 000 g mol<sup>-1</sup>. The nominal flow rate of all the eluents was 0.9 mL min<sup>-1</sup>. The mass of H40 and its fractions injected onto the column was (1–3)  $\times 10^{-3}$  g, whereas the solution concentration was typically (1–3)  $\times 10^{-2}$  g mL<sup>-1</sup>. The calculation of  $\bar{M}_w$  from MALS requires a sample specific refractive index increment ( $dn/dc$ ), which was determined from the DR response assuming a sample mass recovery from the column of 100%. Data acquisition and evaluation utilized Astra 4.73.04 software (Wyatt Technology Corp.). Since a MALS detector is not particularly sensitive toward low molar mass species, the sample molar mass averages were recalculated using Corona 1.40 software (Wyatt Technology Corp.), where the scattered data points at the end of the chromatogram were fitted by regression.<sup>27</sup>

H40 was fractionated in DMAc using a PLgel 10  $\mu$ m Mixed-D preparative column (300 mm length and 25 mm i.d.; effective molar mass range: 200 g mol<sup>-1</sup> to 400 000 g mol<sup>-1</sup>; Polymer Laboratories, Ltd). The mass injected into the preparative column was 0.1 g (solution concentration of 5  $\times 10^{-2}$  g mL<sup>-1</sup>) and the flow rate of the eluent was 2.3 mL min<sup>-1</sup>.

The <sup>1</sup>H (300 MHz) and <sup>13</sup>C (75 MHz) NMR spectra were recorded on a Varian VXR 300 NMR spectrometer using DMSO-*d*<sub>6</sub> as a solvent and tetramethylsilane (TMS) as an internal reference. <sup>13</sup>C NMR spectra were obtained using 10% solutions (except for fraction F3, where the solution concentration was only 2% due to an insufficient amount of the sample) using an inverse gated decoupling mode with a suppressed NOE effect (a relaxation delay of 20 s, an acquisition time of 5 s and up to 20 000 repetitions). <sup>1</sup>H NMR spectra were recorded for solutions with a concentration of 0.5% both at room temperature and at 75 °C (a relaxation delay of 20 s, an acquisition time of 5 s and up to 500 repetitions).

Electrospray ionization-mass spectrometry (ESI–MS) measurements were performed on a LCQ ion trap mass spectrometer (Finnigan, MAT) with an electrospray ionization (ESI) interface. A mixture of 0.1 vol % ammonia in methanol/water (0.8:0.2, v/v) was used as the mobile phase with a flow-rate of 0.5 mL min<sup>-1</sup>. The injection volume was 50  $\mu$ L. The ESI–MS conditions were as follows: capillary temperature 250 °C, ion time 5.00 ms, sheath gas flow pressure (N<sub>2</sub>) 0.8 MPa, auxiliary gas flow pressure (N<sub>2</sub>) 0.2 MPa, source voltage 4.50 kV, source current 1.60  $\mu$ A, capillary voltage 10.00 V, and tube lens offset 10.00 V. A negative scan was obtained at *m/z* values from 150.0 to 2000.0.

Differential scanning calorimetry (DSC) measurements were made using a Pyris 1 Perkin-Elmer DSC apparatus with Al pans at heating/cooling rates of 10 and 200 °C min<sup>-1</sup>, respectively. The glass transition temperature  $T_g$  was obtained from the second heating scan.

## 3. Results

**3.1. SEC-MALS. 3.1.1. *N,N*-Dimethylacetamide (DMAc).** A major problem encountered in the molar mass determination of hyperbranched polyester polyols is the solubility of the samples on a molecular level. In DMAc, the observed molar mass distribution of H40 is multimodal (Figure 1A). The intensity of the light scattering (LS) signal increases with decreasing scattering angle (Figure 1B), indicating that high molar mass associates (clusters) are present in the DMAc solution.<sup>28</sup> As a consequence, the sample molar mass averages are greatly overestimated and the molar mass distribution is very broad. The molar mass averages increase with increasing solute concentration indicating a higher degree of aggregation (Table 1). In the investigated concentration range, the value of  $\bar{M}_n$  is about 10 times higher and  $\bar{M}_w$  about 10<sup>3</sup> times higher than the theoretical molar mass of an ideal fourth generation hyperbranched polyester polyol ( $M_{\text{theor}} = 7316$  g mol<sup>-1</sup>).

The shape of the differential refractometer (DR) response changes with concentration as well. When a lower solute amount (solution concentration = 7.06  $\times 10^{-3}$  g mL<sup>-1</sup>, injected volume 100  $\mu$ L) is injected, the DR response has two poorly resolved peaks, which merge with increasing concentration into one broad peak with a very high molar mass (solution concentration = 2.76  $\times 10^{-2}$  g mL<sup>-1</sup>; injected volume 100  $\mu$ L), (Figure 2, Table 1). To better understand the structure-to-molar mass distribution relationship, we collected three fractions of H40 (denoted as F1, F2, and F3) at the outlet of a preparative column as shown in Figure 3. Fractions F1, F2, and F3 represent about 20%, 70%, and 10% of the whole H40 sample. Collected fractions were first evaporated and then dried in a vacuum oven



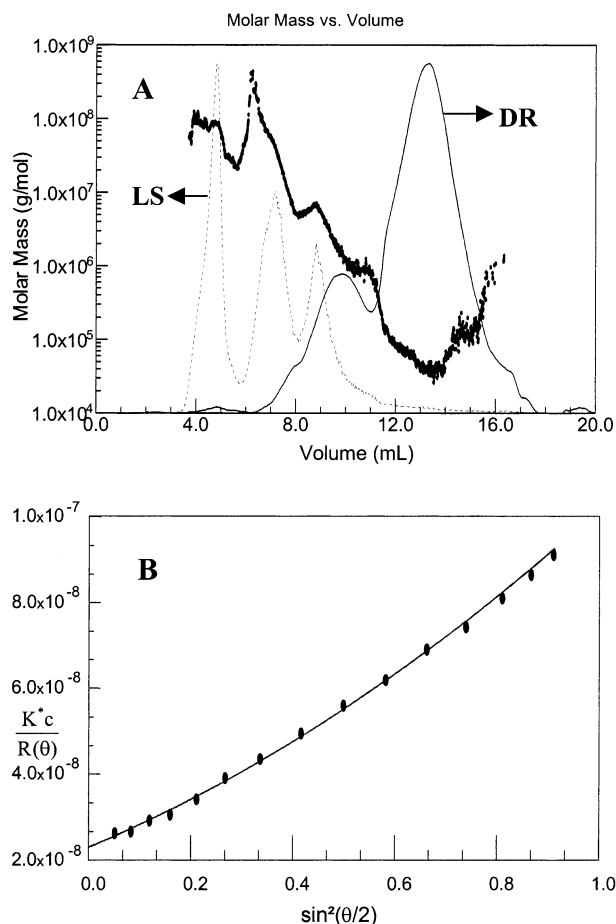


**Figure 1.** (A) Molar mass as a function of elution volume and the SEC-MALS chromatogram of H40 in DMAc. Key: injected mass =  $7.06 \times 10^{-4}$  g, injection volume =  $100 \mu\text{L}$ ,  $\bar{M}_n = 8.3 \times 10^4$  g mol $^{-1}$ ,  $\bar{M}_w = 1.5 \times 10^6$  g mol $^{-1}$ , PDI = 18 (---) LS response at  $90^\circ$ ; (—) DR response). (B) Intensity of the scattered light vs angle for H40 in DMAc.

**Table 1.** SEC-MALS Results for H40 in DMAc, 0.7% LiBr/DMAc,<sup>a</sup> and THF/MeOH (9:1)<sup>a</sup>

injected mass (g)	$\bar{M}_w$ (g mol $^{-1}$ )	$\bar{M}_n$ (g mol $^{-1}$ )	$\bar{M}_w/\bar{M}_n$	$dn/dc$ (mL g $^{-1}$ )
DMAc				
$7.060 \times 10^{-4}$	$1.5 \times 10^6$	$8.3 \times 10^4$	18	0.063
$2.046 \times 10^{-3}$	$2.1 \times 10^6$	$1.6 \times 10^5$	13	0.063
$2.761 \times 10^{-3}$	$2.6 \times 10^6$	$2.2 \times 10^5$	12	0.063
0.7% LiBr/DMAc				
$1.532 \times 10^{-3}$	6620	2430	2.72	0.065
$1.800 \times 10^{-3}$	6560	2660	2.47	0.065
$2.079 \times 10^{-3}$	6730	2650	2.54	0.065
THF/MeOH (9:1)				
$1.816 \times 10^{-3}$	6820	2635	2.59	0.074
$2.418 \times 10^{-3}$	6870	2580	2.66	0.074
$2.996 \times 10^{-3}$	6880	2660	2.59	0.074

<sup>a</sup> Molar mass averages were calculated using Corona software.

at  $75^\circ\text{C}$ . H40 and its fractions were characterized by NMR, SEC-MALS, and DSC techniques.

### 3.1.2. 0.7% LiBr/DMAc and THF/MeOH (9:1, v/v).

The dissolution of H40 on a molecular level was achieved in 0.7% LiBr/DMAc and THF/MeOH (9:1, v/v). The detailed procedure for preparing sample solutions without aggregation will be described in a forthcoming paper.<sup>27</sup> The molar mass averages and molar mass distribution of H40 in both solvents were determined at three different solution concentrations. The calculated  $dn/dc$  are independent of solution concentration

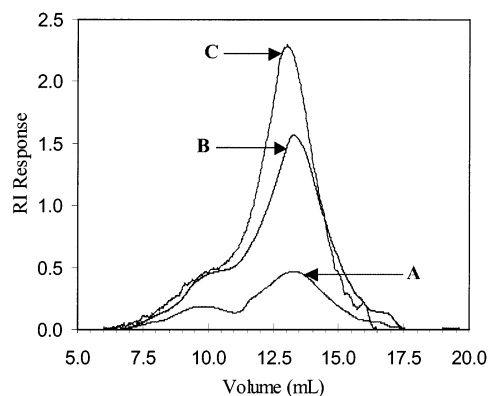


**Figure 2.** Differential refractometer chromatograms of H40 in DMAc at three different concentrations injected:  $A = 7.06 \times 10^{-3}$  g mL $^{-1}$ ,  $B = 2.05 \times 10^{-2}$  g mL $^{-1}$ ,  $C = 2.76 \times 10^{-2}$  g mL $^{-1}$ ; injected volume =  $100 \mu\text{L}$ .

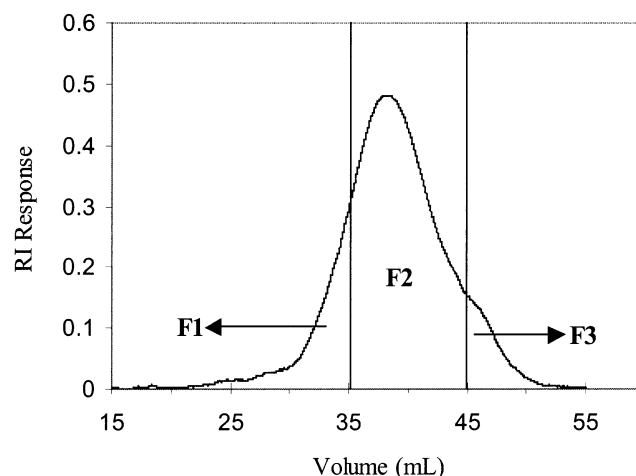


**Figure 3.** Differential refractometer chromatogram of H40 in DMAc obtained using a preparative Mixed-D column. Solution concentration:  $5 \times 10^{-2}$  g mL $^{-1}$ . Injected volume: 2 mL. Fraction 1 = 20–35 min, fraction 2 = 35–45 min, and fraction 3 = 45–55 min.

(Table 1), thus indicating complete mass recovery of the sample from the column. In both solvents, LS responses skewed toward high molar masses indicate a broad molar mass distribution of H40 (Figure 4, parts A and C). The intensity of the scattered light does not change with scattering angle (Figure 4, parts B and D), which is indicative of small particles.<sup>28</sup> Since the LS detector is not particularly sensitive toward low molar mass species at the end of the chromatogram<sup>29</sup> (in Figure 4A, elution volumes  $>8.7$  mL and in Figure 4C, elution volumes  $>16.6$  mL), the sample  $\bar{M}_n$ , which is governed above all by low molar mass species, is overestimated and, consequently, the sample polydispersity is underestimated. To obtain reliable data on the  $\bar{M}_n$  and PDI values of the samples, the scattered data points at the end of the chromatograms were fitted with the regression curve using Corona software.<sup>30</sup> In both solvents, the molar mass averages of H40 are comparable and independent of solution concentration, thus indicating no aggregation of H40 (Table 1).

DR chromatograms of the fractions in both solvents show that they elute from the column in the same order as in DMAc; i.e., the hydrodynamic volume decreases in the order  $F1 > F2 > F3$  (Figure 5). The SEC-MALS chromatograms of all three fractions in LiBr/DMAc

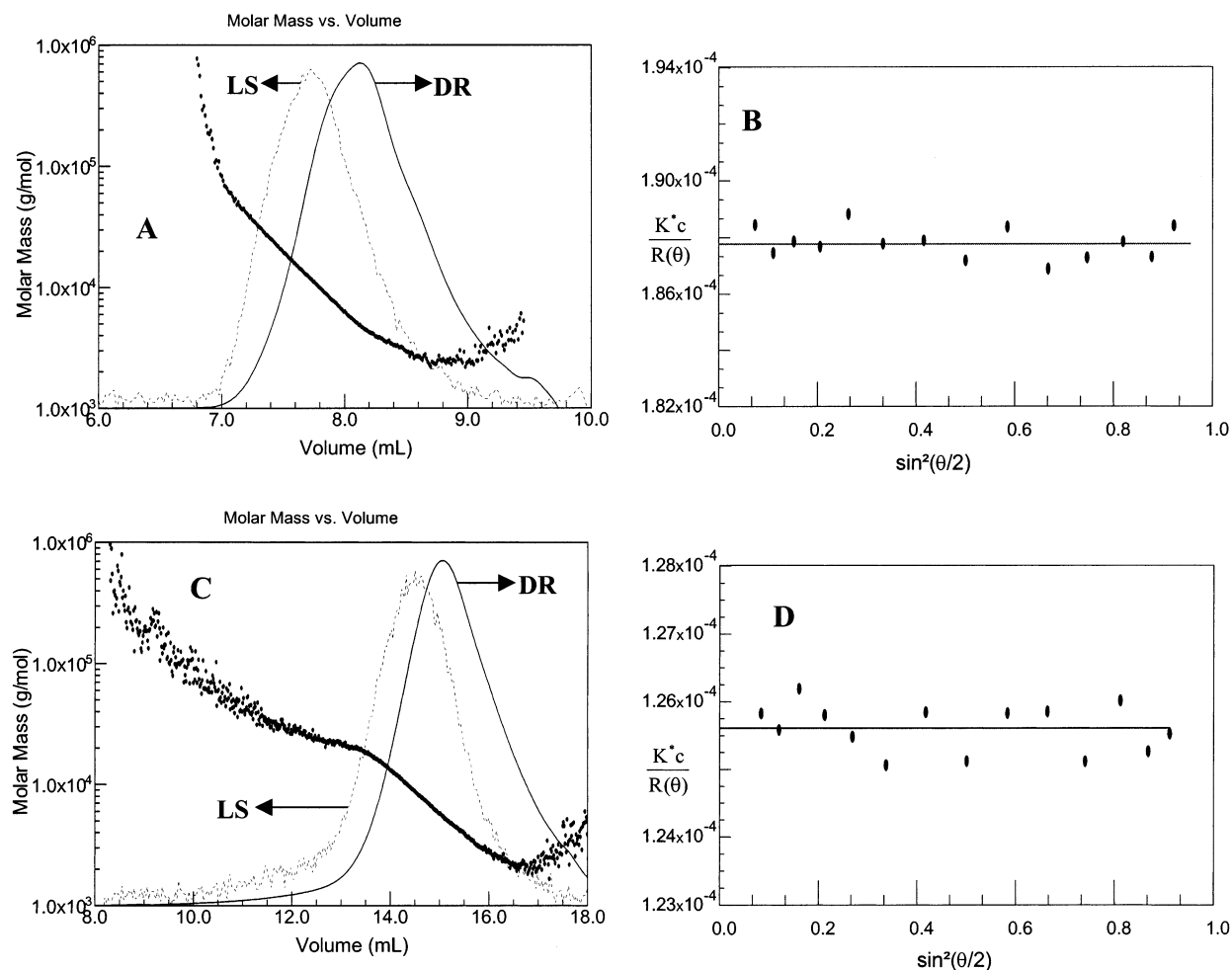


**Figure 4.** Molar mass as a function of elution volume together with SEC-MALS chromatogram of H40 in (A) 0.7% LiBr/DMAc and (C) THF/MeOH (9:1): (---) LS response at angle  $90^\circ$ ; (—) DR response. The intensity of the scattered light vs angle for solutions of H40 in 0.7% LiBr/DMAc (B) and THF/MeOH (9:1) (D).

indicate one asymmetrical peak with a broad molar mass distribution (Figure 6). The  $90^\circ$  light scattering curves of F1 and F3 are skewed considerably toward high molar masses. In a THF/MeOH mixture, DR molar mass distributions are narrower than in LiBr/DMAc (Figure 7). However, LS response of F1 shows an intense peak with an apex at around 9 mL. The DR molar mass distributions of F2 and F3 in THF/MeOH also show a minor peak at a small elution volume (about 9 mL), whereas the major one is at a larger elution volume (F2 at about 15.4 mL and F3 at about 16.4 mL). An intense  $90^\circ$  LS signal of the first peak barely detected by the DR detector indicates a minute fraction of fairly high molar mass species. In both solvents,  $\bar{M}_n$  decreases from F1 to F3, whereas  $\bar{M}_w$  and PDI values decrease in the order  $F1 > F3 > F2$ . The molar mass distributions of F1 and F3 are broader than that of F2, which is the only one with a PDI comparable to that of H40 (Table 2). Contrary to H40 sample, the values of the molar mass averages of individual fractions in both solvents somewhat differ.

**3.2. NMR Spectroscopy. 3.2.1.  $^{13}\text{C}$  NMR.** In the  $^{13}\text{C}$  NMR spectra of H40 (Figure 8) and its fractions, the methyl groups of poly(bis-MPA) resonate at around 17 ppm, quaternary carbons in the region 45–51 ppm, methylene groups between 62 and 66 ppm, and carbonyl groups between 171 and 175 ppm. The signals at around 70 ppm are due to the ether groups of the ethoxylated

**Table 2.** SEC-MALS Results for Fractions (F1, F2, F3) of H40 in 0.7% LiBr/DMAc and THF/MeOH (9:1)<sup>a</sup>

fraction	$\bar{M}_w$ (g mol <sup>-1</sup> )	$\bar{M}_n$ (g mol <sup>-1</sup> )	$\bar{M}_w/\bar{M}_n$
0.7% LiBr/DMAc			
F1	60 000	10 000	6.0
F2	7000	2400	2.9
F3	10 100	2300	4.4
THF/MeOH (9:1)			
F1	44 500	8700	5.1
F2	10 500	3700	2.8
F3	14 400	3500	4.1

<sup>a</sup> Molar mass averages were calculated using Corona software.

core molecule PP50. The individual groups of poly(bis-MPA) resonate at somewhat different chemical shifts, reflecting the kind of repeat unit, generation number, and position in different conformers.<sup>17,20,21</sup>

The dependence of the chemical shift on the kind of repeat unit can be distinctly seen in the region of the quaternary carbons (Figure 9).<sup>17,19</sup> From the quantitative proton-decoupled  $^{13}\text{C}$  NMR spectra the relative fractions of the individual repeat units in H40 and its fractions were determined by comparing the integrals of the quaternary carbon signals belonging to the terminal ( $\delta = 50.2$  ppm), linear ( $\delta = 48.2$  ppm) and dendritic ( $\delta = 46.2$  ppm) units.  $^{13}\text{C}$  NMR spectra reveal that H40 and fractions F2 and F3 also contain "focal point" acid units or acid dendritic units<sup>19</sup> ( $\delta = 45.6$  ppm),

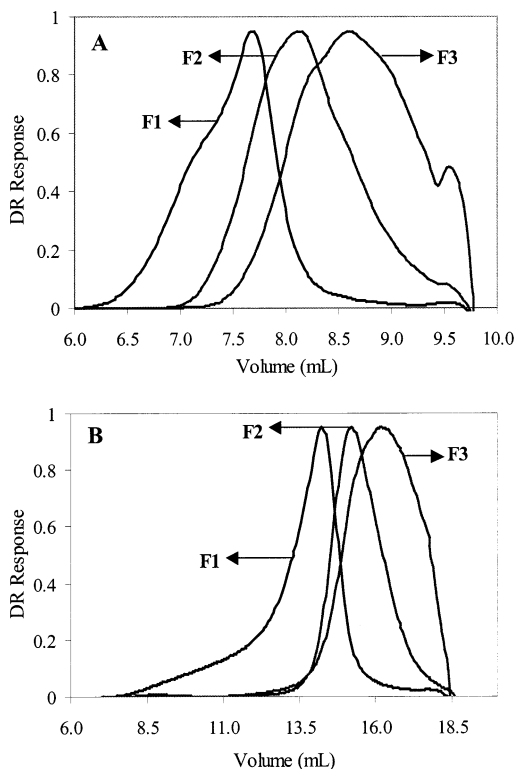


**Figure 5.** DR chromatograms of fractions (F1, F2, F3) in (A) 0.7% LiBr/DMAc and (B) THF/MeOH (9:1).

**Table 3.** Content of Dendritic (D), Linear (L), and Terminal (T) Repeat Units, Degree of Branching (DB), and the Average Number Degree of Polymerization ( $\overline{DP}_n$ ) of H40 and Its Fractions (F1, F2, F3) Determined by  $^{13}\text{C}$  NMR Spectroscopy

parameter	H40	F1	F2	F3
$D_{\text{expt}}$ (%)	16.5	17.5	16.0	13.5
$D_F$ (%)	23.0	25.0	24.0	23.0
$L_{\text{expt}}$ (%)	57.0	59.0	57.0	58.0
$L_F$ (%)	50.0	50.0	50.0	49.9
$T_{\text{expt}}$ (%)	26.5	23.5	27.0	28.5
$T_F$ (%)	27.0	25.0	26.0	27.1
DB(eq 1) <sup>a</sup> (%)	43.0	41.0	43.0	42.0
DB(eq 2) <sup>b</sup> (%)	36.7	37.2	36.0	31.8
$\text{DB}_p^c$ (%)	48.5	50.0	49.0	48.0
$\Delta[\text{DB}_p - \text{DB}(\text{eq } 2)]$ (%)	11.8	12.8	13.0	16.2
$\overline{DP}_n$ (eq 9)	21	62	21	14

<sup>a</sup> DB = degree of branching according to Fréchet.<sup>10</sup> <sup>b</sup> DB = degree of branching according to Frey.<sup>11</sup> <sup>c</sup>  $\text{DB}_p = p_A/2$  coefficient of branching determined from the conversion of bis-MPA carboxyl groups;<sup>13</sup>  $p_A$  = conversion of bis-MPA carboxyl groups. <sup>d</sup>  $D_{\text{expt}}$ ,  $L_{\text{expt}}$ , and  $T_{\text{expt}}$  are fractions of dendritic, linear, and terminal repeat units determined experimentally from  $^{13}\text{C}$  NMR spectra.  $D_F$ ,  $L_F$ , and  $T_F$  are fractions of individual repeat units calculated by equations presented by Frey et al.<sup>12</sup>

where the quaternary carbon is attached to an unreacted acid group and two reacted hydroxyl groups. The spectrum of fraction F1 shows additional quaternary carbon signals of low intensity at about 47.20 and 49.25 ppm. These signals were assigned to dendritic and linear units, which differ from regular ones in that they contain one ether group.<sup>23</sup> The compositions and DBs determined according to eqs 1 and 2 for H40 and its fractions are collected in Table 3.

The  $\overline{DP}_n$  can also be calculated from the intensities of the quaternary carbon signals for individual structural units in the  $^{13}\text{C}$  NMR spectra of poly(bis-

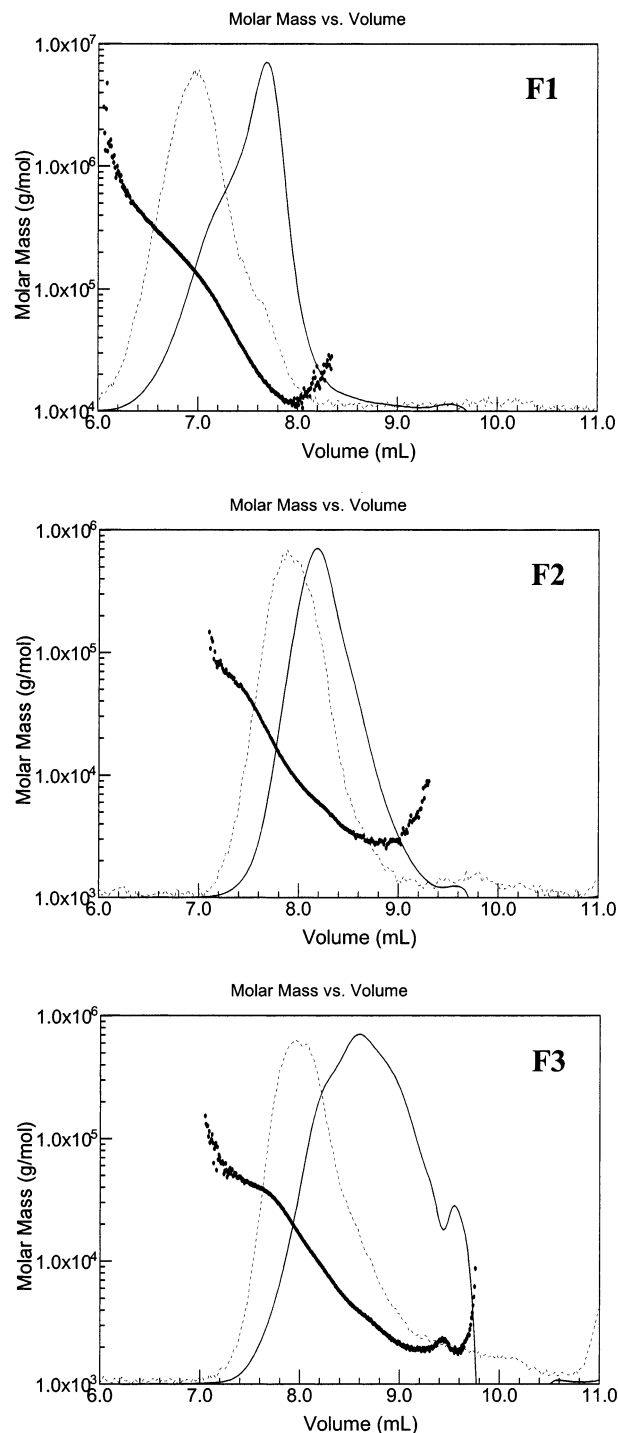


**Figure 6.** Molar mass as a function of elution volume together with SEC-MALS chromatograms for fractions (F1, F2, F3) of H40 in 0.7% LiBr/DMAc: (---) LS response at angle 90°; (—) DR response.

MPA).<sup>11,31,32</sup> In this calculation we take into account the amount of deactivated bis-MPA carboxyl groups (eq 9)

$$\overline{DP}_n = \left( \frac{T + L + D}{T - D} \right) x_{B_4} f + \left( \frac{T + L + D}{T - D} \right) x_{B_2} \quad (9)$$

where  $f$  is the functionality of the core molecule ( $f = 4$  for PP50) and  $x_{B_4}$ ,  $x_{B_2}$  are the fractions of  $B_4$  and  $B_2$  core molecules (eq 17). The calculated  $\overline{DP}_n$  values from  $^{13}\text{C}$  NMR spectra are collected in Table 3.

**3.2.2.  $^1\text{H}$  NMR.** The calculation of  $\overline{DP}_n$  for poly(bis-MPA) with tris(methylol)propane or PP50 core molecule

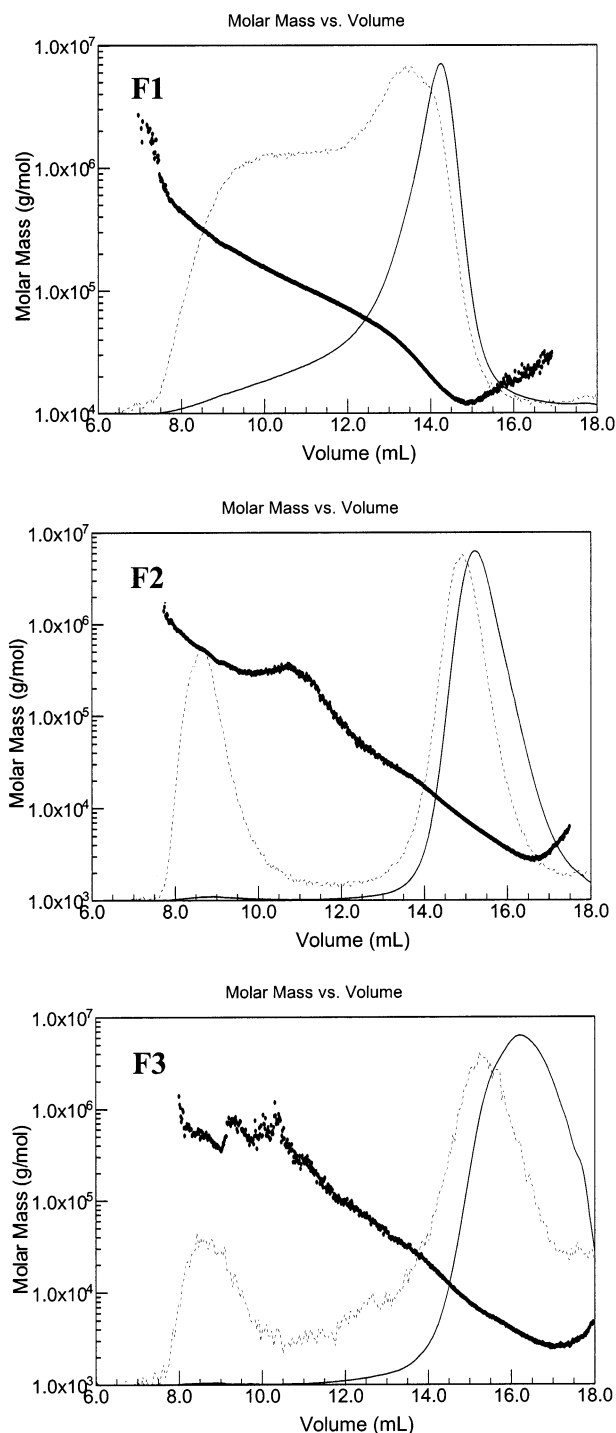


**Figure 7.** Molar mass as a function of elution volume together with SEC-MALS chromatograms for fractions (F1, F2, F3) of H40 in THF/MeOH (9:1): (---) LS response at angle  $90^\circ$ ; (—) DR response.

using  $^1\text{H}$  NMR spectroscopy has been described by Frey et al. (eq 7).<sup>22</sup> We extended this calculation further and will show that the fraction of a core molecule, deactivated bis-MPA carboxyl groups and the fraction of ether groups can also be determined from  $^1\text{H}$  NMR spectra. Knowing the fraction of deactivated A groups allows us to calculate the  $\text{DP}_n$  as discussed below. Since the intensities of the signals for individual groups of poly-(bis-MPA) are crucial for determining  $\text{DP}_n$ ,  $\bar{M}_n$ , and the fractions of core molecule, deactivated carboxyl

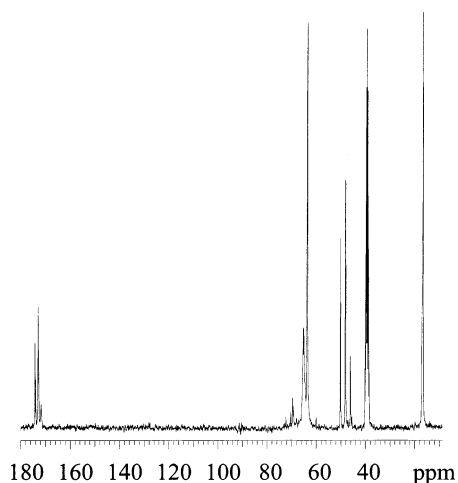


**Figure 8.**  $^{13}\text{C}$  NMR spectrum of H40 in  $\text{DMSO}-d_6$  at a solution concentration of 10 wt %.

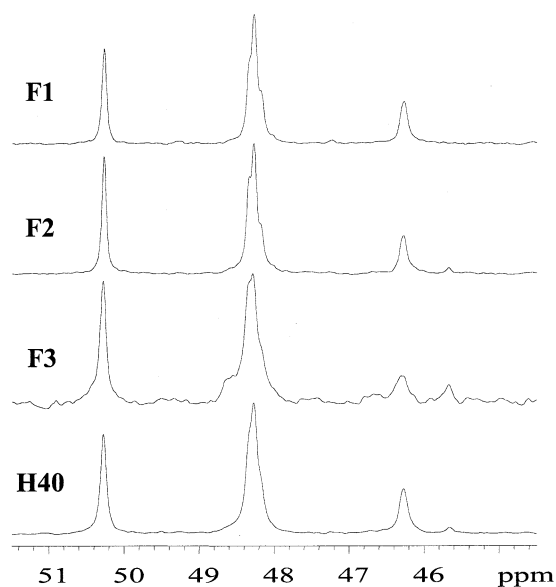


**Figure 9.**  $^{13}\text{C}$  NMR spectra of H40 and its fractions in  $\text{DMSO}-d_6$ . Quaternary carbon region of the spectra was magnified.

groups, and ether groups, the  $^1\text{H}$  NMR spectra must be recorded under quantitative experimental conditions. Therefore, the solution concentration was 0.5 wt %, the dissolution time was at least 2 days, and the delay time was 20 s.

In the  $^1\text{H}$  NMR spectra of H40 (Figure 10B), the protons of the methyl group in the terminal, linear and dendritic repeat units resonate at 1.02, 1.07, and 1.17 ppm, respectively.<sup>23</sup> Contrary to the quaternary carbon signals, the methyl signals are broad and poorly resolved. Fractions F2 and F3 show additional signals for methyl groups between 1.12 and 1.15 ppm, whose relative intensities are the highest in F3 (Figure 11). From the composition determined by  $^{13}\text{C}$  NMR and the fact that these signals approach the signal of methyl groups in the linear repeat units with increasing temperature, these signals have been ascribed to methyl groups in the linear repeat units.

The protons of the unreacted carboxyl groups ( $-\text{COOH}$ ) of bis-MPA resonate at 12–13 ppm. The intensity of this signal increases from fraction F1 to fraction F3 (Table 4). The methylene groups in

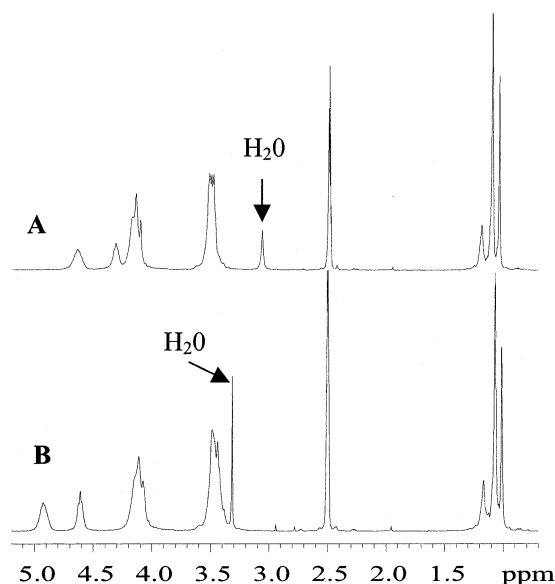


**Figure 10.**  $^1\text{H}$  NMR spectra of H40 in  $\text{DMSO}-d_6$  at solution concentration of 0.5 wt %: (A) = 75 °C; (B) room temperature.

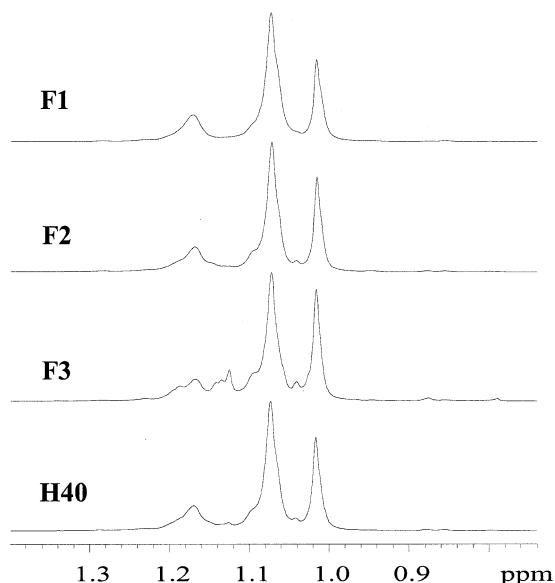


**Figure 11.**  $^1\text{H}$  NMR spectra of H40 and its fractions in  $\text{DMSO}-d_6$ . Magnification of the methyl region of the spectra.

**Table 4. Integrals of the  $^1\text{H}$  NMR Signals of Individual Groups for Boltorn H40 and its fractions (F1, F2, F3)**

group	H40	F1	F2	F3
Integrals of the $^1\text{H}$ Signals of Individual Groups				
$I(\text{CH})$	54.11	52.82	54.18	56.37
$I(\text{CH}_2\text{OR})$	35.00	35.17	35.15	36.06
$I(\text{CH}_2\text{OH})$	46.08	42.71	46.98	50.02
$I(\text{OH})$	19.77	18.30	19.96	21.11
$I(\text{COOH})$	0.22		0.21	0.35
Calculated Values				
$I(\text{CH}_2)_{\text{Penta}}$ (eq 13)	2.55	2.13	2.82	3.12
$I(\text{CH}_2)_{\text{EO}}$ (eq 13)	6.38	5.32	7.06	7.80
$N_{B_2}$ (eq 13)	0.46	<i>a</i>	0.49	0.76

<sup>a</sup>  $N_{B_2}$  cannot be determined from eq 15 since it is a negative value.

the vicinity of reacted hydroxyl groups ( $-\text{CH}_2\text{OR}$ ) resonate at approximately 4.2 ppm, whereas the methylene groups attached to the unreacted hydroxyl groups ( $-\text{CH}_2\text{OH}$ ) resonate at approximately 3.5 ppm

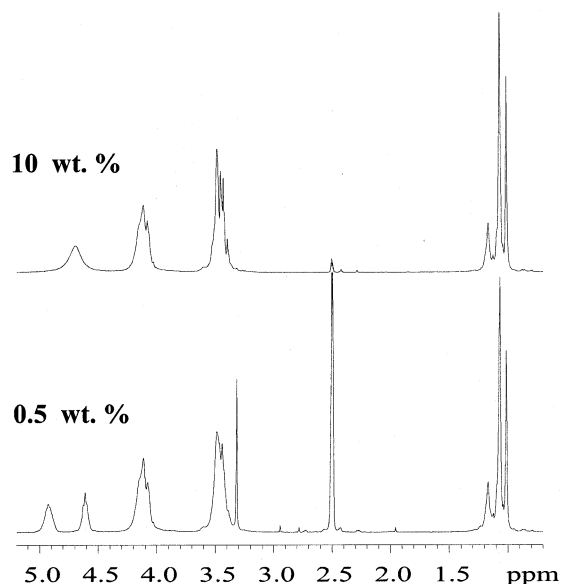


**Figure 12.**  $^1\text{H}$  NMR spectra of H40 in  $\text{DMSO}-d_6$  at solution concentration of 10 wt % or 0.5 wt %.

(Figure 10). At room temperature, the chemical shift of  $-\text{CH}_2\text{OH}$  coincides with that of the  $\text{H}_2\text{O}$  protons (Figure 10B). However, at elevated temperatures, i.e., 75 °C, the signal of water at 3.07 ppm is well separated from the signal for  $-\text{CH}_2\text{OH}$  at 3.5 ppm (Figure 10A). Therefore, the integral value of the signal for  $-\text{CH}_2\text{OH}$  at room temperature was determined by comparing the integrals of the signals for  $-\text{CH}_2\text{OH}$  and  $-\text{CH}_3$  groups at room temperature and at 75 °C (eq 10).

$$I(\text{CH}_2\text{OH})_{\text{RT}} = I(\text{CH}_3)_{\text{RT}} I(\text{CH}_2\text{OH})_{75^\circ\text{C}} / I(\text{CH}_3)_{75^\circ\text{C}} \quad (10)$$

At high solution concentrations (10 wt % in Figure 12A), the apex of the broad signal for the protons of the hydroxyl groups appears at 4.5 ppm. At a concentration of 0.5 wt %, there are two well-resolved signals situated at 4.61 and 4.93 ppm (Figure 12B). The signal at 4.61 ppm resonates at the same frequency as the protons of end hydroxyl groups in the ideal dendrimer from bis-MPA<sup>21</sup> and was therefore ascribed to the hydroxyl groups of terminal repeat units, whereas the signal at 4.93 ppm was ascribed to the protons of hydroxyl groups in the linear repeat units. At a low solution concentration, all hydroxyl groups are well solvated and the difference in the chemical shifts is due to the different chemical environment. Namely, hydroxyl groups in linear repeat units are in the vicinity of two electron-withdrawing ester groups, while those in terminal units are in the vicinity of an ester and a hydroxyl group. At higher concentrations, the signal at 4.93 ppm moves to a higher magnetic field, presumably because of the solvent inaccessibility to the linear repeat units in the interior layers. The hydroxyl groups in the linear units are therefore most probably H-bonded with the ester carbonyl groups.

The Boltorn HX hyperbranched polyester polyols were synthesized using PP50 as a core molecule without a methyl group in the structure (Scheme 1). The fraction of PP50 can be estimated from the  $^1\text{H}$  NMR spectra in the following way. Taking into account that each methyl group of bis-MPA and poly(bis-MPA), respectively, is surrounded by two methylene groups, either attached to the reacted ( $-\text{CH}_2\text{OR}$ ) or unreacted ( $-\text{CH}_2\text{OH}$ ) hy-



droxyl groups, the calculated integral corresponding to poly(bis-MPA) methylene groups  $I(\text{CH}_2)_{\text{calcd}}$  is

$$I(\text{CH}_2)_{\text{calcd}} = \frac{4}{3}I(\text{CH}_3) \quad (11)$$

where  $I(\text{CH}_3) = I(\text{CH}_3)_D + I(\text{CH}_3)_L + I(\text{CH}_3)_T$  is the sum of the integrals of poly(bis-MPA) methyl groups in the  $^1\text{H}$  NMR spectra belonging to dendritic, linear, and terminal units, respectively. When the core molecule (PP50) is without a methyl group, the difference between the actual integral value for methylene groups  $I(\text{CH}_2)$  and the calculated poly(bis-MPA) methylene groups  $I(\text{CH}_2)_{\text{calcd}}$  (eq 11), is represented by the integral of the methylene groups of the core molecule

$$I(\text{CH}_2)_{B_4} = I(\text{CH}_2) - I(\text{CH}_2)_{\text{calcd}} \quad (12)$$

where  $I(\text{CH}_2) = I(\text{CH}_2\text{OH}) + I(\text{CH}_2\text{OR})$  is the sum of the integrals of poly(bis-MPA) methylene groups near unreacted  $I(\text{CH}_2\text{OH})$  and reacted  $I(\text{CH}_2\text{OR})$  hydroxyl groups.

Since the PP50 core molecule contains an average of five ethylene oxide units per Pentaerythritol (5 EO/Penta),<sup>18</sup> whose chemical shift coincides with that of the  $-\text{CH}_2\text{OH}$  groups, the fractions of the core  $-\text{CH}_2-$  groups belonging to EO ( $I(\text{CH}_2)_{\text{EO}}$ ) and Penta ( $I(\text{CH}_2)_{\text{Penta}}$ ) can be calculated according to eq 13.

$$I(\text{CH}_2)_{\text{Penta}} = \frac{2I(\text{CH}_2)_{B_4}}{7} \quad \text{and} \quad I(\text{CH}_2)_{\text{EO}} = \frac{5I(\text{CH}_2)_{B_4}}{7} \quad (13)$$

If etherification as a side reaction does not occur during polymerization,  $N(B)$ ,  $N(\text{AB})$  and  $N_{\text{core}}$  in eq 7 can be substituted with  $I(\text{OH})$ ,  $(1/2)I(\text{CH}_2\text{OR})$  and  $(1/4)I(\text{CH}_2)_{\text{Penta}}$ , respectively. Thus, eq 7 transforms into eq 14.

$$\overline{\text{DP}}_n = \frac{2I(\text{OH}) + I(\text{CH}_2\text{OR}) - \frac{1}{2}I(\text{CH}_2)_{\text{Penta}}}{2I(\text{OH}) - I(\text{CH}_2\text{OR}) - \frac{1}{2}I(\text{CH}_2)_{\text{Penta}}} \quad (14)$$

The  $\overline{\text{DP}}_n$  of hyperbranched polyester polyols can also be calculated using another approach. If we assume an ideal experiment,<sup>14</sup> where all of the added  $\text{AB}_2$  molecules react only with the growing core molecules  $B_4$ , the number of core molecules  $B_4$  is equal to the number of macromolecules eventually formed. Thus, the ideal hyperbranched molecule has  $\overline{\text{DP}}_n = X + 1$  ( $X$  is a monomer/core ratio), meaning that there are on average  $X$  monomer units per core molecule. The number of hydroxyl groups is  $X + 4$ , since each added  $\text{AB}_2$  monomer raises the total number of available functionalities of the core by 1.

In a nonideal case, the A group in the  $\text{AB}_2$  monomer is deactivated and this  $\text{AB}_2$  monomer thus represents a new  $B_2$  core molecule, which yields a macromolecule composed of  $M\text{AB}_2$  monomers with one A group and  $(M + 1)B$  groups. If new  $B_2$  core molecules are formed in the course of the reaction, the number of macromolecules is no longer equal to the number of  $B_4$  core molecules, but increases with an increasing fraction of deactivated  $\text{AB}_2$  monomers. Therefore,  $\overline{\text{DP}}_n$  and the number of hydroxyl groups is no longer equal to  $X + 1$  and  $X + 4$ , respectively, but decrease with increasing deactivation of the A groups in the  $\text{AB}_2$  monomer.<sup>14</sup> The

number of deactivated A groups is identical to the number of the additional, newly formed  $B_2$  core molecules. The fraction of macromolecules without the core molecule can be determined from  $^1\text{H}$  NMR spectra as follows.

If we presume that side reactions, i.e., the etherification and cyclization through ester groups, do not occur during the polymerization, the difference between the actual integral value of the signals for hydroxyl groups and the calculated theoretical value of hydroxyl groups of the ideal hyperbranched polyester, is equal to the fraction of the newly formed  $B_2$  core molecules  $N_{B_2}$

$$N_{B_2} = I(\text{OH}) - (4N_{B_4} + N_{\text{bis-MPA}}) = I(\text{OH}) - \left[ \frac{I(\text{CH}_2)_{\text{Penta}}}{2} + \frac{I(\text{CH}_3)}{3} \right] \quad (15)$$

where  $N_{B_4} = I(\text{CH}_2)_{\text{Penta}}/8$  is the fraction of PP50 core molecule and  $N_{\text{bis-MPA}} = I(\text{CH}_3)/3$  the fraction of monomer units.  $I(\text{OH})$  and  $I(\text{CH}_3)$  are the integrals of the signals for the  $-\text{OH}$  and  $-\text{CH}_3$  groups of poly(bis-MPA), and  $I(\text{CH}_2)_{\text{Penta}}$  is the calculated integral of the PP50  $-\text{CH}_2-$  groups near the reacted or unreacted hydroxyl groups, respectively.

When the A group of  $\text{AB}_2$  monomer is deactivated, the total number of macromolecules in the reaction mixture is equal to the sum of  $B_4$  (eq 13) and  $B_2$  (eq 15) core molecules. Therefore, the average number of monomer molecules per core molecule  $X$  is calculated by eq 16.

$$X = \frac{N_{\text{bis-MPA}}}{N_{B_4} + N_{B_2}} = \frac{I(\text{CH}_3)/3}{\frac{I(\text{CH}_2)_{\text{Penta}}}{8} + I(\text{OH}) - \left( \frac{I(\text{CH}_2)_{\text{Penta}}}{2} + \frac{I(\text{CH}_3)}{3} \right)} \quad (16)$$

The fractions of  $B_4$  and  $B_2$  core molecules  $x_{B_4}$ ,  $x_{B_2}$  are

$$x_{B_4} = \frac{N_{B_4}}{N_{B_4} + N_{B_2}} \quad \text{and} \quad x_{B_2} = \frac{N_{B_2}}{N_{B_4} + N_{B_2}} = 1 - x_{B_4} \quad (17)$$

The  $\overline{\text{DP}}_n$ , which takes into account the fraction of  $B_4$  core molecules, can be expressed by eq 18.

$$\overline{\text{DP}}_n = \frac{N_{\text{bis-MPA}}}{N_{B_4} + N_{B_2}} + \frac{N_{B_4}}{N_{B_4} + N_{B_2}} = \frac{8I(\text{CH}_3) + 3I(\text{CH}_2)_{\text{Penta}}}{24I(\text{OH}) - 9I(\text{CH}_2)_{\text{Penta}} - 8I(\text{CH}_3)} \quad (18)$$

The number-average molar masses  $\bar{M}_n$  of H40 and its fractions are calculated using eq 19.

$$\bar{M}_n = (\overline{\text{DP}}_n - 1)(M_{\text{bis-MPA}} - M_{\text{H}_2\text{O}}) + x_{B_4}M_{B_4} + x_{B_2}M_{B_2} = 116(\overline{\text{DP}}_n - 1) + 356x_{B_4} + 134x_{B_2} \quad (19)$$

Equation 19 takes into account the amount and molar mass of the core molecules.

If the etherification side reaction does not occur during polymerization of bis-MPA, the sample  $\overline{\text{DP}}_n$  values calculated in these two different ways (eqs 14 and 18) are equal. They are also equal, but overesti-

**Table 5. Average Number Degree of Polymerization ( $\overline{DP}_n$ ) (Eqs 14 and 18), the Average Number of bis-MPA Molecules Per One Core Molecule ( $X$ , Eq 16), Number Average Molar Mass ( $\overline{M}_n$ ) (Eq 19), the Fraction of Hyperbranched Macromolecules with and without Core Molecules ( $x_{B_4}$ ,  $x_{B_2}$ , Eq 17), the Portion of  $B_4$  Core Molecules (%  $B_4$ ), the Portion of Bis-MPA Deactivated Carboxyl Groups (%  $\text{COOH}_{DA}$ ), the Conversion of Bis-MPA Carboxyl Groups ( $p_A$ ), the Fraction of Ether Groups (% Ether), and the Average Number of Hydroxyl Groups per One Hyperbranched Macromolecule (OH) for Boltorn H40 and Its Fractions (F1, F2, F3)**

parameter	H40	F1	F2	F3
$\overline{DP}_n$ (eq 14)	22.44	193.71	21.92	16.68
$\overline{DP}_n$ (eq 18)	23.75	67.13	21.85	16.68
$X$ (eq 16)	23.16	66.13	21.44	16.34
$\overline{M}_n$ (eq 19)	2864		2647	2028
$x_{B_4}$ (eq 17)	0.41	1	0.42	0.34
$x_{B_2}$ (eq 17)	0.59	0	0.58	0.66
% $B_4^a$			1.92	2.04
% $(\text{COOH})_{DA}^b$			2.3	4.0
$p_A^c$			0.98	0.96
% ether <sup>d</sup>	0.4	2.1		
OH <sup>e</sup>			23.69	18.36

<sup>a</sup> %  $B_4 = x_{B_4}/(x_{B_4} + X)$ , the portion of core molecule PP50 in hyperbranched polyester. <sup>b</sup> %  $-\text{COOH}_{DA} = (x_{B_2}/X) \times 100$ , the portion of deactivated  $-\text{COOH}$  groups of bis-MPA. <sup>c</sup>  $p_A = (X - x_{B_2})/X$ , the conversion of A groups of  $AB_2$  monomer. <sup>d</sup> % ether, the fraction of etherified hydroxyl groups. <sup>e</sup> % OH =  $X + 4x_{B_4} + x_{B_2}$ , the average number of  $-\text{OH}$  functional groups per one hyperbranched macromolecule.

mated to the same extent when the A group of the focal unit reacts with the B group of the same molecule to form a cycle (loop), i.e., an intramolecular esterification. In the first case, the total conversion obtained from  $^1\text{H}$  NMR is higher, whereas in the second case the calculated amount of  $B_2$  core molecules (eq 15) is underestimated. Actually, this side reaction does not increase  $\overline{DP}_n$ .

If etherification (intra- or intermolecular) as a side reaction takes place during the polymerization, then the  $\overline{DP}_n$  values calculated in these two different ways (eqs 14 and 18) differ. Two hydroxyl groups are consumed in the formation of the ether group ( $-\text{CH}_2-\text{O}-\text{CH}_2-$ ). The methylene protons of the ether groups resonate at the same frequency as protons of methylene groups near the unreacted hydroxyl groups ( $-\text{CH}_2\text{OH}$ ).

Regarding H40 and its fractions, the  $\overline{DP}_n$  values obtained by eqs 14 and 18 agree well for fractions F2 and F3, whereas for H40 they somewhat differ (Table 5). The  $\overline{DP}_n$  (eq 14) of fraction F1 is unexpectedly high compared to the  $\overline{DP}_n$  calculated by eq 18 (Table 5). The calculated theoretical value of hydroxyl groups is higher than the actual integral for hydroxyl groups  $I(\text{OH})$ . Therefore, the fraction of  $B_2$  core molecules (eq 15) cannot be determined for F1 (Table 4). To find out whether the reason for the discrepancy between both  $\overline{DP}_n$  in the case of H40 and F1 is actually the etherification, the integral for hydroxyl groups  $I(\text{OH})_{\text{calcd}}$  was calculated from the integral for the methylene groups near the unreacted hydroxyl groups  $I(\text{CH}_2\text{OH})$  after the fraction of  $\text{EO}-\text{CH}_2-$  groups of PP50 core molecule have been subtracted (eq 20).

$$I(\text{OH})_{\text{calcd}} = \frac{1}{2}(I(\text{CH}_2\text{OH}) - I(\text{CH}_2)_{\text{EO}}) \quad (20)$$

The  $I(\text{OH})_{\text{calcd}}$  (Table 6) value for H40 and fraction F1 is larger than the actual integral for hydroxyl groups

$I(\text{OH})$  (Table 4) ( $I(\text{OH})_{\text{calcd}} > I(\text{OH})$ ), indicating that a small fraction of hydroxyl groups react in ether groups during the polymerization of H40. If etherification occurs intermolecularly, an additional bis-MPA unit is built up in the polymer structure as in the case of intermolecular esterification. Therefore, this side reaction increases the  $\overline{DP}_n$  of the final product. In contrast, intramolecular etherification does not increase  $\overline{DP}_n$ , but only increases cyclization. In the case of intermolecular etherification, the accurate  $\overline{DP}_n$  is obtained if we presume that half of the etherified hydroxyl groups,  $1/2(I(\text{OH})_{\text{calcd}} - I(\text{OH}))$ , react intermolecularly with carboxyl groups. In the case of intramolecular etherification, the accurate  $\overline{DP}_n$  is obtained if we use  $I(\text{OH})_{\text{calcd}}$  in the calculation instead of  $I(\text{OH})$ . By recalculation of  $\overline{DP}_n$  using eqs 14 and 18 for H40 and F1 considering etherification as intramolecular reaction, both  $\overline{DP}_n$ s agree very well (Table 6).

## 4. Discussion

**4.1. Composition.** With increasing conversion of bis-MPA carboxyl groups, the fraction of dendritic units increases and the fraction of terminal repeat units decreases (Table 3, Figure 9), which is consistent with the evolution of these repeat units according to the equations derived by Frey et al.<sup>12</sup> For the fractions of H40, the portion of linear repeat units decreases in the order  $F1 > F3 > F2$  (Table 3). Compared to the model,<sup>12</sup> assuming equal reactivities of both kinds of hydroxyl groups, our experimental data show a higher fraction of linear and smaller fraction of dendritic repeat units for all fractions (Table 3). This means that the reaction of an acid group with a terminal hydroxyl group to form a linear repeat unit is favored compared to the statistical case, since terminal hydroxyl group is more reactive than that in linear unit ( $k_1 > k_2$ ).<sup>18</sup> This could be due to changes in reactivity when one of the hydroxyl groups has reacted and/or due to the hindered accessibility of hydroxyl groups in the linear repeat units. The presence of focal acid dendritic units in  $^{13}\text{C}$  NMR spectra of H40 and its fractions (Figure 9) reveals that bis-MPA reacted not only with the growing  $B_4$  core molecule but also with another bis-MPA monomer to form hyperbranched structures without the core molecules. This is especially evident for fraction F3 (Table 5). Since the reaction most probably proceeds not only by the addition of monomer to the growing macromolecule, but also between the oligomers, the content of linear repeat units in fraction F3 is unexpectedly high, despite the carboxyl group conversion is the lowest. However, this is probably because the hydroxyl groups in the linear repeat units are less accessible, especially for reaction with focal unit carboxyl groups, due to the bulkiness of the hyperbranched structure.<sup>19</sup>

**4.2. Degree of Branching (DB).** The negative substitution effect of the bis-MPA/PP50 system is reflected in the DB values (eqs 1 and 2) of H40 and its fractions, which are much smaller than the values of DB calculated from the conversion of carboxyl groups of bis-MPA,  $\text{DB}_p = p_A/2$  (Table 3). The DB of fractions determined by eq 1 range between 0.41 and 0.43 and do not change substantially with conversion. The values of DB determined by eq 2 increase with increasing conversion (Table 3). In addition, at a given conversion, the values of DB according to these definitions differ. This is because the DB values obtained by eq 1 decrease

**Table 6. Recalculation of Parameters Quoted in Table 5 for H40 and Its Fraction F1 Considering Etherification (Intra- and Intermolecular) as a Side Reaction**

parameter	H40		F1	
	intramolecular etherification	intermolecular etherification	intramolecular etherification	intermolecular etherification
$I(CH_2OR)$	35.00	35.04	35.17	35.37
$I(OH)_{\text{calcd}}$ (eq 20)	19.85	19.85	18.70	18.70
$\overline{DP}_n$ (eq 14)	21.44	21.70	61.90	75.07
$\overline{DP}_n$ (eq 18)	21.37	21.37	61.36	61.36
$X$ (eq 16)	21.00	21.00	60.45	60.45
$\bar{M}_n$ (eq 19)	2579		7338	
$x_{B_4}$ (eq 17)	0.37		0.91	
$x_{B_2}$ (eq 17)	0.63		0.09	
% $B_4^a$	1.73		1.48	
% $(COOH)_{DA}^b$	3.0		0.15	
$p_A^c$	0.97		1.00	
% $OH^d$	22.97 <sup>d</sup>		62.82 <sup>d</sup>	

<sup>a</sup> %  $B_4 = x_{B_4}/(x_{B_4} + X)$ , the portion of core molecule PP50 in hyperbranched polyester. <sup>b</sup> %  $-COOH_{DA} = (x_{B_2}/X) \times 100$ , the portion of deactivated  $-COOH$  groups of bis-MPA. <sup>c</sup>  $p_A = (X - x_{B_2})/X$ , the conversion of A groups of  $AB_2$  monomer. <sup>d</sup> The average of  $-OH$  functional groups per one hyperbranched molecule:  $OH = X + 4x_{B_4} + x_{B_2}$ ; the etherified  $-OH$  groups were subtracted from the calculated number of  $-OH$  groups.

from 1 ( $p_A = 0$ ) to 0.5 at full conversion, whereas the DB obtained by eq 2 increases from zero ( $p_A = 0$ ) to 0.5.<sup>10,11,33</sup>

Hult et al.<sup>19</sup> reported that the DB of a hyperbranched polyester is enhanced to  $DB_{eq2} = 0.44$  by adding discrete fractions of bis-MPA corresponding to each generation to the core molecule tris(methylol)propane with a functionality of  $f = 3$  (a stepwise or "pseudo-generation-wise" addition). Increased DB was attributed to the higher accessibility of carboxyl groups of continuously dissolved bis-MPA in tris(methylol)propane melt, compared to the carboxyl groups of bulky focal units. Our results show that H40 has a lower DB ( $DB_{eq2} = 0.367$ ,  $p_A = 0.97$ ) than that of poly(bis-MPA) with core molecule tris(methylol)propane, and a comparable DB to poly(bis-MPA) without the core molecule obtained via standard one-pot polymerization ( $DB_{eq2} = 0.37$ ,  $p_A = 0.96-0.98$ ).<sup>19</sup> Considering spatial constraints, which affect the probability of functional group reacting, it is not surprising that the hydroxyl groups of linear repeat units in hyperbranched macromolecules growing from a functionality 4 core are less reactive than those in the hyperbranched structure with the functionality 3 core. Namely, spatial constraints are in proportion to segment density, which increases with increasing core functionality.<sup>14</sup>

The enhancement in DB of the hyperbranched polyester by pseudo-generation-wise addition of  $AB_2$  monomers to the core molecule has no theoretical support.<sup>12</sup> This type of monomer addition is classified as a repeat one-pot procedure and as such it is highly unlikely that a bulk polymerization will satisfy the slow addition/dilution conditions. This is especially true when amounts equivalent to higher generations are added to the reaction mixture.

**4.3. Degree of Polymerization and Molar Mass Characteristics.** Since the pseudo-generation-wise addition of bis-MPA to PP50 core molecule does not satisfy the core-dilution/slow addition conditions, some of the bis-MPA carboxyl groups are deactivated, thus preventing their reaction with the growing core molecules. Because of this deactivation the fraction of macromolecules having low molar masses is higher than without deactivation. Accordingly,  $\bar{M}_n$  of H40 is significantly lower than the theoretical molar mass (Tables 1, 3, and 6), while  $\bar{M}_w$  is influenced only slightly (Table 1).

As a consequence, the PDI of H40 is larger (2.6, Table 1) than it would be when there is no deactivation ( $PDI = 1 + 1/f = 1.25$ ).<sup>14,15</sup> Despite deactivation the PDI of H40 is reduced compared to that of poly(bis-MPA) without the core molecule ( $PDI = 5.7$ ).<sup>18</sup> The reason for the reduced PDI is that the bis-MPA/PP50 system reacts with a negative substitution effect. A rate constant for the reaction of carboxyl groups of bis-MPA with the hydroxyl groups of the core ( $k_0$ ) is higher than rate constants for the reaction of carboxyl groups with hydroxyl groups in the terminal ( $k_1$ ) or linear ( $k_2$ ) repeat units of poly(bis-MPA) ( $k_0 > k_1, k_2$ ).<sup>34-36</sup> Hult et al.<sup>18</sup> attributed the high reactivity of PP50 as being due to phase separation of the reaction mixture during polyesterification, which is performed at a reaction temperature (140 °C) well above the melting point of PP50 (mp < 25 °C) and below that of bis-MPA (mp = 180–190 °C). Therefore, the bis-MPA is continuously solubilized in the PP50 melt, which enhances the probability of the reaction of bis-MPA carboxyl groups with the hydroxyl groups of the core.

Experimentally determined  $\bar{M}_n$  of H40 using SEC–MALS along with a regression (Table 1) agrees very well with the calculated  $\bar{M}_n$  from the  $^1H$  NMR spectrum (Table 6). These results indicate that the aggregation of H40 through H-bonding was successfully prevented. Moreover, comparable calculated and experimental  $\bar{M}_n$  values in both solvents indicate that the elution of the sample is governed by a size exclusion mechanism. From these results, we also infer that the intramolecular esterification (cyclization) is not an important side reaction in the case of H40. Namely, it is highly unlikely that the increase in the experimentally determined  $\bar{M}_n$  due to aggregation is the same as the increase in calculated  $\bar{M}_n$  due to an overestimated conversion as a consequence of cyclization via ester groups.

Comparison of  $\overline{DP}_n$  values calculated from eq 14 and 18 indicates that etherification as a side reaction takes place during the polymerization of H40 to a very small extent (below 1%, Table 5). The amount of ether groups in H40 is much lower compared to that determined for poly(bis-MPA) without the core molecule.<sup>23</sup> Out of all the fractions, F1, with the highest carboxyl groups conversion, contains the highest amount of ether groups (Table 5). Ether groups are most probably formed during intramolecular cyclization.



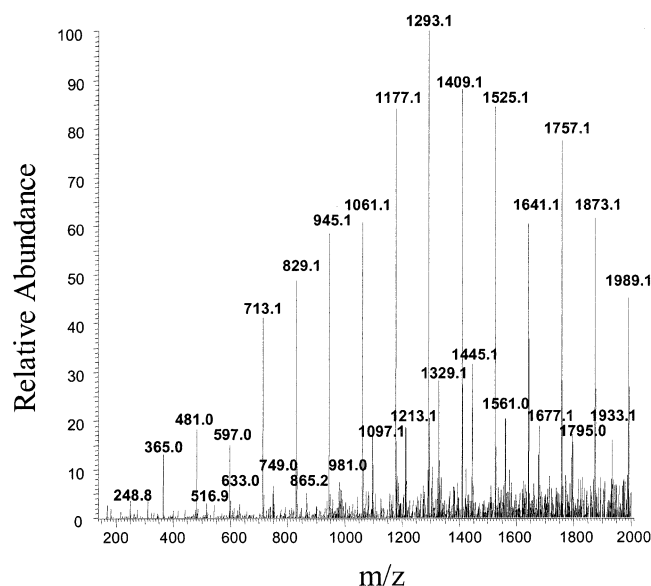


**Figure 13.** ESI/MS of H40, negative ionization. The peaks of higher intensity correspond to the acyclic structures without the core molecule and the peaks of lower intensity to the acyclic structures with core molecule PP50.

To determine the cyclic species in H40, ESI-MS was used to distinguish between the molecular ions of acyclic and cyclic species. In the mass spectrum of H40, the main peaks are the molecular ions of acyclic species with deactivated carboxyl groups and without a core molecule (Figure 13). The molar masses of the acyclic species without a core molecule can be calculated using eq 21.

$$M = \text{DP}_n M_{\text{bis-MPA}} - (\text{DP}_n - 1) M_{\text{H}_2\text{O}} \quad (21)$$

In addition to the main distribution, signals of lower intensity appear in the mass spectra and have been ascribed to the desired species attached to the PP50 core molecule. Both distributions possess a distance of 116 between the two peaks, which corresponds to the repeat unit  $M_{\text{bis-MPA}} - M_{\text{H}_2\text{O}}$ , as expected. The mass spectrum of H40 indicates that the intensity of the signals due to cyclic species with molar masses  $M = \text{DP}_n(M_{\text{bis-MPA}} - M_{\text{H}_2\text{O}})$  is very low. From the mass spectra, it is not possible to distinguish whether cyclic structures result from etherification or esterification, since both reactions result in the elimination of a water molecule. These results and the fact that  $\bar{M}_n$  obtained by SEC-MALS and  $^1\text{H}$  NMR are comparable indicate that the content of cyclic structures in H40 is low and that they are formed through intramolecular etherification rather than intramolecular esterification.

Frey et al.<sup>22</sup> also investigated Boltorn hyperbranched polyester polyols, but they did not evidence for cyclic structures. The difference in the content of cyclic structures in poly(bis-MPA) with a tris(methylol)propane core molecule and H40 with a PP50 core molecule could be due to a different carboxyl group conversions. Unfortunately, the conversion of carboxyl groups in poly(bis-MPA) with tris(methylol)propane was not reported in the article.

$\overline{\text{DP}}_n$  and consequently  $\bar{M}_n$  obtained from the  $^1\text{H}$  NMR spectra decrease from F1 to F3 (Table 5 for F2 and F3 and Table 6 for F1). The highest  $\overline{\text{DP}}_n$  comparable to the theoretical value ( $\overline{\text{DP}}_n = 61$ ) is only

**Table 7.** Glass Transition Temperatures ( $T_g$ ) of H40 and Its Fractions (F1, F2, F3)

	H40/DMAc	F1	F2	F3
$T_g/^\circ\text{C}$	25	39	21	10

characteristic of F1 ( $\overline{\text{DP}}_n = 62$ ). F2 and F3 have much lower  $\overline{\text{DP}}_n$  values due to deactivation of the bis-MPA carboxyl groups. Therefore, the fraction of macromolecules without a core molecule increases from F1 to F3 on account of the decreasing fraction of hyperbranched macromolecules with PP50 core molecule (Tables 5 and 6). This agrees with the increasing amount of focal point acid units in the same order as shown in the quaternary carbon region of the  $^{13}\text{C}$  NMR spectra of the fractions (Figure 9) and in the increasing integral value of the signal for  $-\text{COOH}$  groups in the  $^1\text{H}$  NMR spectra (Table 4). The number of hydroxyl groups per molecule decreases in the same order as the  $\overline{\text{DP}}_n$  (Table 5, 6).

The SEC-MALS results for the H40 fractions, conversely to those of the entire sample, indicate that some of the macromolecules aggregated. This is seen in the SEC-MALS chromatograms with intense LS responses of the species eluted from the column at lower elution volumes (Figures 6 and 7) and also in the average molar masses and PDI values (Table 2). Namely, experimental  $\bar{M}_n$  values are higher than calculated ones. The only exception is fraction F2 in LiBr/DMAc, where both  $\bar{M}_n$  values are comparable. Nevertheless, the experimental and the calculated  $\bar{M}_n$  decreases from F1 to F3. Contrary to  $\bar{M}_n$ ,  $\bar{M}_w$  and therefore also PDI decrease in the order  $\text{F1} > \text{F3} > \text{F2}$ , thus indicating that aggregation especially impacts  $\bar{M}_w$  values and to a lesser extent  $\bar{M}_n$  values (Table 2). The reason for the high molar masses of fractions obtained by SEC-MALS is such that during the drying of samples at temperatures above their glass transitions, more stable aggregated structures were formed<sup>37,38</sup> in which H-bonding was not completely prevented under the experimental conditions used for breaking down the aggregated structures in the preparation of the sample solutions for SEC-MALS measurements.<sup>27</sup>

The increase in molar mass from F1 to F3 is also reflected in an increasing glass transition temperature ( $T_g$ ) in the same order (Table 7). Namely, the increase in  $T_g$  is a consequence of the skeleton buildup as the molar mass increases.<sup>39</sup> It should be noted that the  $T_g$  values of fractions are affected by the plasticization effect of the DMAc trapped in the hyperbranched structure to a certain extent. This is also evidenced from the  $T_g$  value of the H40 sample, which had been previously dissolved in DMAc and further dried according to the procedure described for the fractions. Thus, the  $T_g$  decreases from 34  $^\circ\text{C}$  for the original sample to 25  $^\circ\text{C}$  for the sample dissolved in DMAc.

## 5. Conclusion

The most important side reaction in the synthesis of the Boltorn H40 fourth generation hyperbranched polyester polyol is the deactivation of bis-MPA carboxyl groups. The fraction of deactivated carboxyl groups decreases with increasing molar mass. This deactivation lowers  $\bar{M}_n$  for H40 considerably compared to its theoretical molar mass, while the  $\bar{M}_w$  is influenced only slightly. This is reflected in the sample's PDI, which is higher than it would be without deactivation. Despite deactivation, comparison of the molar masses and the



PDI for H40 and poly(bis-MPA) without the core molecule synthesized via one pot synthesis indicates that the stepwise addition of bis-MPA to PP50 core molecule permits to control of the sample molar mass and PDI. The results of the composition determination reveal that the DB is not enhanced by the addition of PP50 core molecules.

Another much less important side reaction for the analyzed hyperbranched polyester is intramolecular etherification, which results in cyclic structures. The comparable  $\bar{M}_n$  values obtained by SEC-MALS and the  $^1\text{H}$  NMR spectrum and the mass spectrum of H40 reveal that intramolecular esterification, which also leads to cyclic structures, most probably did not occur during the polymerization of H40.

**Acknowledgment.** We acknowledge financial support by the Ministry of Education, Science, and Sport of the Republic of Slovenia (Program P0-514-104).

## References and Notes

- (1) (a) Tomalia, D. A.; Baker, H.; Dewald, J. R.; Hall, M.; Kallos, G.; Martin, S.; Roeck, J.; Ryder, J.; Smith, P. *Polym. J. (Tokyo)* **1985**, *17*, 117. (b) Tomalia, D. A.; Naylir, A. M.; Goddard, W. A. *Angew. Chem., Int. Ed. Engl.* **1990**, *29*, 138.
- (2) Brabender, E. M. M.; Meijer, E. W. *Angew. Chem., Int. Ed. Engl.* **1993**, *32*, 1308.
- (3) (a) Newkome, G. R.; Yao, Z.; Baker, G. R.; Gupta, V. K. *J. Org. Chem.* **1985**, *50*, 2003. (b) Newkome, G. R.; Moorfield, C. N.; Baker, G. R. *Aldrichim. Acta* **1992**, *25*, 31.
- (4) Buhlein, E.; Wehner, W.; Vögtle, F. *Synthesis* **1978**, 155.
- (5) Mishra, M. K.; Kobayashi, S. *Star and Hyperbranched Polymers*; Marcel Dekker: New York, 1999.
- (6) (a) Fréchet, J. M. J. *Science* **1994**, *263*, 1710. (b) Hawker, C. J.; Farrington, P. J.; McKay, M. E.; Wooley, K. L.; Fréchet, J. M. J. *J. Am. Chem. Soc.* **1995**, *117*, 4409. (c) Fréchet, J. M. J.; Henmi, M.; Gitsov, I.; Aoshima, S.; Leduc, M. R.; Grubbs, R. B. *Science* **1995**, *269*, 1080. (d) Kim, Y. H.; Webster, O. W. *Macromolecules* **1992**, *25*, 5561. (e) Kim, Y. H.; Beckerbauer, R. *Macromolecules* **1994**, *27*, 1968. (f) Kim, Y. H. *J. Polym. Sci., Part A: Polym. Chem.* **1998**, *36*, 1685. (g) Mourey, T. H.; Turner, S. R.; Rubinstein, M.; Fréchet, J. M. J.; Hawker, C. J.; Wooley, K. L. *Macromolecules* **1992**, *25*, 2401. (h) Wooley, K. L.; Fréchet, J. M. J.; Hawker, C. J. *Polymer* **1994**, *35*, 4489.
- (7) Hult, A.; Johansson, M.; Malmström, E. *Adv. Polym. Sci.* **1999**, *143*, 1.
- (8) Sunder, A.; Heinemann, J.; Frey, H. *Chem.—Eur. J.* **2000**, *6*, 2499.
- (9) Malmström, E.; Hult, A. *J. Macromol. Sci.—Rev. Macromol. Chem. Phys.* **1997**, *C37* (3), 555.
- (10) Hawker, C. J.; Lee, R.; Fréchet, J. M. J. *J. Am. Chem. Soc.* **1991**, *113*, 4583.
- (11) Hölter, D.; Burgath, A.; Frey, H. *Acta Polym.* **1997**, *48*, 30.
- (12) Hölter, D.; Frey, H. *Acta Polym.* **1997**, *48*, 298.
- (13) Flory, P. J. *J. Am. Chem. Soc.* **1952**, *74*, 2718.
- (14) Hanselmann, R.; Hölter, D.; Frey, H. *Macromolecules* **1998**, *31*, 3790.
- (15) Radke, W.; Litvinenko, G.; Müller, A. H. E. *Macromolecules* **1998**, *31*, 239.
- (16) Hawker, C.; Chu, F. *Macromolecules* **1996**, *29*, 4370.
- (17) Malmström, E.; Johansson, M.; Hult, A. *Macromolecules* **1995**, *28*, 1698.
- (18) Malmström, E.; Hult, A. *Macromolecules* **1996**, *29*, 1222.
- (19) Magnusson, H.; Malmström, E.; Hult, A. *Macromolecules* **2000**, *33*, 3099.
- (20) Ihre, H.; Hult, A.; Söderlind, J. *Am. Chem. Soc.* **1996**, *118*, 6388.
- (21) Ihre, H.; Hult, A.; Fréchet, J. M. J.; Gitsov, I. *Macromolecules* **1998**, *31*, 4061.
- (22) Burgath, A.; Sunder, A.; Frey, H. *Macromol. Chem. Phys.* **2000**, *201*, 782.
- (23) Komber, H.; Ziemer, A.; Voit, B. *Macromolecules* **2002**, *35*, 3514.
- (24) Flory, P. J. *Principles of Polymer Chemistry*; Cornell University Press: Ithaca, NY, 1953.
- (25) Dušek, K.; Šomvárský, J.; Smrčková, M.; Simonsick, W. J.; Wilczek, L. *Polym. Bull. (Berlin)* **1999**, *42*, 489.
- (26) Certificate of Boltorn H40 Analysis, Perstorp Specialty Chemicals AB, 2001.
- (27) Žagar, E.; Žigon, M. Article in preparation.
- (28) Kratochvil, P. *Classical light scattering from polymer solutions*; Elsevier: Amsterdam, 1987; Chapter 6.4.
- (29) Wyatt, P. J. *Anal. Chim. Acta* **1993**, *272*, 1.
- (30) Corona Software 1.40 (User's guide), Wyatt Technology Deutschland GmbH, 1996.
- (31) Sunder, A.; Hanselmann, R.; Frey, H.; Mülhaupt, R. *Macromolecules* **1999**, *32*, 4246.
- (32) Sunder, A.; Mülhaupt, R.; Frey, H. *Macromolecules* **2000**, *33*, 309.
- (33) Beginn, U.; Drohmann, C.; Möller, M. *Macromolecules* **1997**, *30*, 4112.
- (34) Galina, H.; Lechowicz, J. B.; Walczak, M. *Macromolecules* **2002**, *35*, 3261.
- (35) Galina, H.; Lechowicz, J. B.; Walczak, M. *Macromolecules* **2002**, *35*, 3253.
- (36) Galina, H.; Lechowicz, J. B. *e-Polymers* **2002**, no. 012.
- (37) Hsieh, T.-T.; Tiu, C.; Simon, G. P. *Polymer* **2001**, *42*, 7635.
- (38) Hult, A.; Malmstrom, E.; Johansson, M. Hyperbranched polyesters. In *Polymeric Materials: Encyclopedia*; Salamon, J. C., Ed.; CRC Press, LLC: Boca Raton, FL, 1996.
- (39) Stutz, H. *J. Polym. Sci., Polym. Phys. Ed.* **1995**, *33*, 333.

MA0210700